POLITECNICO DI MILANO
School of Industrial and Information Engineering
Aerospace Department

Flow on normal flat plates in tandem: Study of the Strouhal number dependence on blockage ratio

by
Marcos Alexander León Ilaño

A dissertation submitted for the degree of
Aeronautical Engineering

Under the supervision of:
Alex Zanotti

Academic year 2018-2019

Acknowledgements

I would like to express my very appreciation to Dr. Alex Zanotti, my thesis supervisor, for his professional guidance, advice and continuous feedback provided during the development of this work. Thanks to his proposal I was able to work with aerodynamics laboratory equipment and make a first approach to the field of research.

I would also like to extend my thanks to Engineer Donato Grassi for his assistance during the experimental activity and the collection of the equipment technical data.

My grateful thanks to the Colegio Mayor San Juan de Ribera for allowing me to study in an excellent environment and grow as a person. My thanks to all the people who constitute this family for making this my second home.

I wish to thank my family for all the support they have always provided to me, particularly these last years. Without their encouragement and care it would not be possible to face this university stage.

Thanks to all the friends I have met during these last years. It has been a pleasure to share unforgettable experiences and work shoulder to shoulder with you.

Thanks to my life-long friends for their patience and support. Despite the distance between us, our bonds are unbreakable.

Finally, a special thank to all the people I met during the Erasmus for making memorable my stay in Milan and more bearable the lectures.

Abstract

The aim of this work is the measurement of flow around flat plates in tandem normal to the free stream using two different blockage ratios. The conducting of the experiments is carried out in a closed return wind tunnel at a fixed Reynolds number $Re = 22400$ with two pairs of plates of different chord in order to change the blockage. The measurements are taken with a hot wire anemometer at the back of the downstream plate for different spacing distances between plates. Thus the relation between the Strouhal number and the separation distance can be found. An additional test is carried out at $Re = 83500$ for a deeper study of the largest blockage.

For a correct visualization of experimental results, it is performed a parametric study of the Fourier Transform representation. From the processed information it can be observed that the blockage ratio significantly affects the Strouhal evolution with the separation distance of the tandem arrangement, whereas the change in Reynolds produces negligible differences. Furthermore, it is noticeable that, unlike to previous experiences, the bistability between two different flow patterns is not shown.

Keywords: Flat plates, tandem, vortex shedding frequency, Strouhal, wind tunnel, blockage ratio, Fourier Transform.

Index

List of Figures

List of Tables

Nomenclature

Lowercase Letters

c	Chord of the plate
f	Vortex shedding frequency
f_s	Sampling frequency
k	Blockage ratio
w	Width of a signal segment

Uppercase Letters

D	Separation distance between plates
L	Characteristic length of a body
M	Number of overlapped points
N	Number of signal segments
N_d	Length of a signal
N_s	Number of points of a signal segment
S_{xx}	Power Spectral density
T	Sampling time
U	Free-stream velocity
AR	Aspect Ratio
CFD	Computational Fluid Dynamics
DFT	Discrete Fourier Transform
FFT	Fast Fourier Transform
FT	Fourier Transform

HWA	Hot wire anemometer
IDFT	Inverse Discrete Fourier Transform
IFT	Inverse Fourier Transform
PSD	Power Spectral Density

Greek Letters

δ	Shift of data points
σ^2	Variance

Dimensionless Numbers

Re	Reynolds number
St	Strouhal number
St_{cor}	Literature Strouhal number for single plate
St_{ref}	Strouhal number for single plate

Other Symbols

Δf	Frequency resolution
$\mathcal{F}$	Fourier Transform function
$\mathcal{F}^{-1}$	Inverse Fourier Transform function
kS	Kilosamples

Chapter 1

Introduction

The study of the flow around several bodies is a significant field within aerodynamics as generally the bodies found in nature do not appear isolated. In fact, the interaction between the wakes produced by bodies can lead to a change in the aerodynamic loads. In some of the literature gathered it is observed that aerodynamic coefficients such as drag and lift coefficients of a body is strongly affected by the presence of another body in its vicinity. Consequently, a deep study must be done for the flow around multiple bodies and the effect of the interactions between them.

The flow around bluff bodies is inherently unsteady, having as main feature the phenomenon widely known as *vortex shedding*. This vortex nature does not allow the use of the potential theory, which assumes irrotational flow, and thus more complex procedures must be followed. CFD allows to solve different unsteady problems with diverse models, which via other means would turn out unreasonable cumbersome. The results which CFD provides are combined with the ones coming from experimental results in order to obtain more reliable conclusions.

Due to the time-dependency of these kind of flows, not only the temporal evolution of aerodynamics forces are of particular interest but also the Strouhal number, a dimensionless number proportional to the frequency.

Due to the complexity of real-world problems, the geometry is usually simplified before solving the tackled problem. This simplification allows to obtain results which are useful as a first approach of the real ones.

The idealization of the shape of the bodies analyzed leads to geometries such as circular, rectangular and square cylinders. These basic geometries can be even combined in order to simulate the ideal interaction of multiple bodies, a more complex case. Within this application the tandem arrangement comes up.

This kind of arrangement fits in the fields of wind engineering and civil engineering. In fact, the flow around a pair of pillars of a bridge and flow around two nearby buildings can be seen as cases of two bodies in tandem.

For tandem configuration it has been demonstrated in previous works for different sections that the Strouhal depends on several factors such as the distance between bodies or the angle of incidence. The previous experience regarding tandem arrangement are studied in more detail in the literature review.

1.1 Literature review

The information regarding the wake produced by bluff bodies which can be found in literature is wide. This issue is particularly interesting as it spans different problems such as the interaction between the wakes of different bodies, the frequency of detachment of vortices in *vortex shedding* and the change of aerodynamic loads in presence of wake.

One of the most studied cases within this field is the case of the wake produced by a flat plate at different angles of incidence. It was firstly faced by [Fage and Johansen, 1927], by measuring the Strouhal number at different Reynolds number and different angle of incidence. Apart from these authors, [Chen and Fang, 1996] not only repeated the same experimental procedure, but found a semi-empirical relation between the Strouhal number and the blockage ratio, based on the model proposed by [Ota et al., 1994].

[Sarpkaya, 1975] tackled the aforementioned case numerically by means of the discrete vortices method. The results obtained were not completely in concordance previous experience: although the Strouhal results were similar, the normal force coefficient were noticeably different to the ones obtained by [Fage and Johansen, 1927].

Furthermore, within this extend field of aerodynamics, is of special interest the configuration of two bodies in tandem since they can lead to complex behavior of the flow. Various geometries of bodies in tandem have been studied in the past: circular cylinders [Zdravkovich, 1977, Igarashi, 1981, Igarashi, 1984, Xu and Zhou, 2004], rectangular [Takeuchi, 1990] and square [Luo et al., 1999]. From the results of theses works, the dependence of the behavior of the flow and the Strouhal number on the distance between the bodies comes up.

The most studied configuration is the case of cylinder with circular section. From the work of [Zdravkovich, 1977] and [Igarashi, 1981, Igarashi, 1984] it is concluded that the Strouhal number forcefully depends on the separation distance, Reynolds number and level of free stream turbulence.

Another tandem configuration with particular interest is the one formed by rectangular cylinders. Some works of interest regarding this configuration are the ones carried out by [Takeuchi, 1990] and [Havel et al., 2001]. The labor of [Takeuchi, 1990] was the research of the stability of bridge pillars, whose section could be cruciform, rectangular or square. On the other hand, the work of [Havel et al., 2001] was focused on the study of flow around a couples of cubes and couples of cylinders with square section, finding four different regimes of flow. Besides, from both works, as it can be observed in Figure 1.1, it is noticeable that exist some cases where the flow exhibits two values of Strouhal number for the same dimensionless distance.

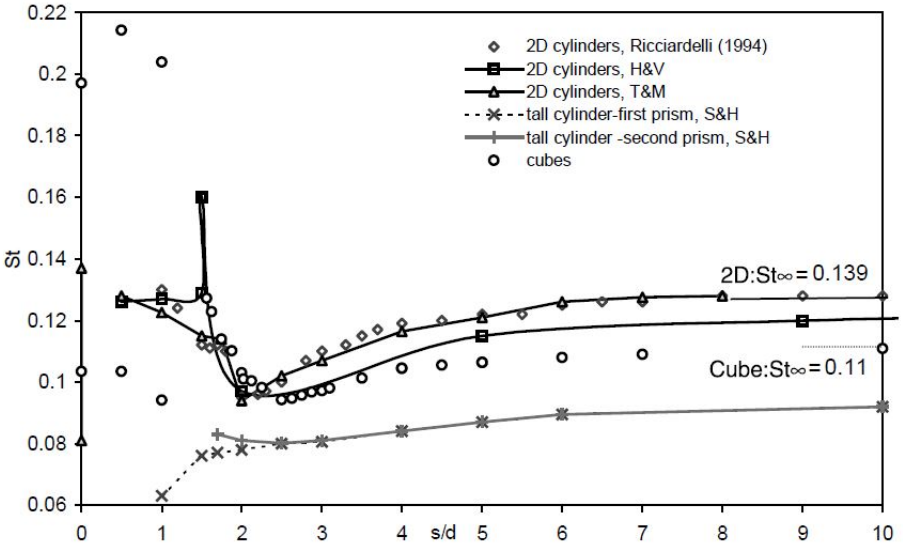

Figure 1.1: Evolution of the Strouhal number as a function of the separation distance in bodies in tandem [Havel et al., 2001]

The research carried out by [Liu and Chen, 2002] is one of the most remarkable as it demonstrates that the Strouhal number of a flow around two square cylinders in tandem depends not only on the distance of separation, but also on the manner this distance is varied. When varying the separation distance is observed the existence of two different flow patterns for a given separation distance within a certain region. The flow pattern produced depends on whether the separation is being increased or decreased. This phenomenon is known as hysteresis. [Liu and Chen, 2002] define two modes for this found hysteresis: *mode I* and *mode II*.

This *mode I* is produced when the shear layers detached from the upstream cylinder reattaches onto the rear cylinder, preventing the *vortex shedding* from the front cylinder. On the other hand, int the *mode II* pattern it is observed that the shear layers separated from the fore cylinder roll up forming vortices in the space between cylinders. In Figure Figure 1.2 it is shown graphically the difference between the two modes. It must be highlighted that these modes are stable and do not switch between them with the course of time.

Another geometry of interest is the normal flat plates instance. This case can be seen as the rectangular cylinder case in the limit when the sides parallel to the flow have no length. In fact, this simplification produces a completely different flow field and eases its study since no complex reattachments and secondary separations are produced.

The literature concerning normal flat plates is reduced. From recent years, it must be highlighted the work carried out by [Grassi, 2002, Auteri et al., 2008, Auteri et al., 2009] from the *Dipartimento di Scienze e Tecnologie Aeroespaziali* (DAER) in Politecnico di Milano. Their measurements for this arrangement are taken at different values of Reynolds numbers, obtaining Strouhal-separation distance curves which collapse in one single curve, thus the independence on the Reynolds number is concluded.

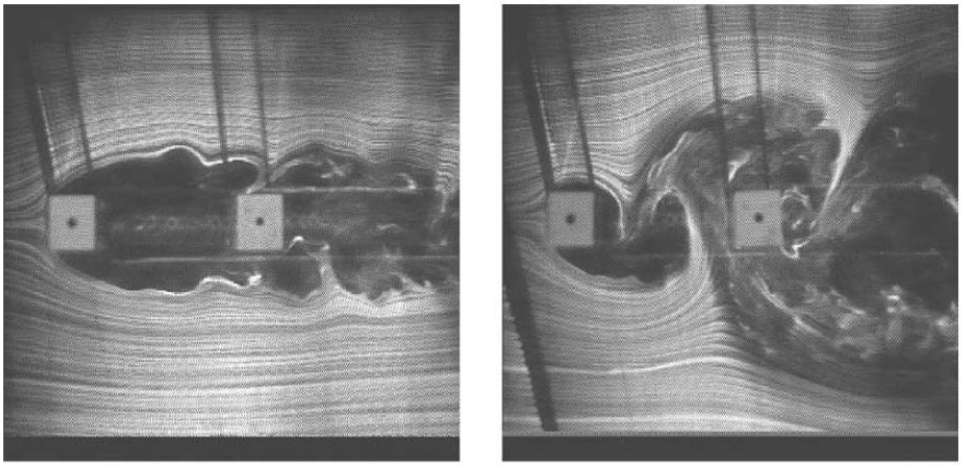

Figure 1.2: The two flow patterns found by [Liu and Chen, 2002] in square cylinders in tandem for $L/D = 4.25$ at $Re = 2700$

From the analysis of the DAER plots, it is found that for a separation distance lower than the chord of the plate the Strouhal number is close to the one of the isolated plate (*mode I*). When the distance is increased the Strouhal increments through a discontinuity, reaching a peak, and immediately it decreases until reaching a minimum for $3 \leq D/c \leq 4$. Subsequently, the Strouhal starts to increase and seems to approach asymptotically to the Strouhal of isolated plate. Once overtaken the aforementioned Strouhal discontinuity, the flow is in the *mode II*. In the zone close to $D/c = 1$, that is, close to the Strouhal peak, the flow is in a state of bistability, continuously switching from one mode to the other in a random way. This bistability condition is in contrast with the result obtained by [Liu and Chen, 2002], in which there is no intermittent change between modes.

Concerning the experimental aspect of the study of flow around bluff bodies, an important parameter to be considered during the experiments is the blockage ratio. Several experiences highlight the effect of this ratio on the flow behavior around a single body[West and Apelt, 1982, Awbi, 1983]. In the work carried out by [Awbi, 1983] it is demonstrated the dependence of the Strouhal on the blockage for circular and rectangular cylinders and [West and Apelt, 1982], apart from showing also the dependence of the Strouhal, prove the clear influence of blockage on pressure distribution and drag coefficient for circular cylinder.

However, the previous experiences only tackle the blockage ratio effect for the cases of single bodies. In fact, the literature addressing the study of flow behavior dependence on blockage ratio for tandem arrangement is nonexistent. The necessity of filling up this gap in the tandem configuration literature justifies a study of the flow around bodies in tandem at different blockage ratios. In particular, the bodies selected for this work are flat plates since they present a quite low thickness which allows to work with a flow particular and easier to be studied.

Furthermore, it is possible to compare the data obtained for one blockage ratio value with other results of the previous work and observe the possible effects of the wind tunnel environment, composed by parameters such as the turbulence level and the three-dimensionality of the flow. With this aim, the results obtained by [Grassi, 2002] are used for the comparison.

The experimental activity of this work follows the same procedure as the literature works: the measurements are taken at different separation distances between the two flat plates. The laboratory work is carried out focusing on the three principal objectives represented in the following points:

- Comparison of the Strouhal evolution for two different blockages in order to observe the effect of blockage.
- Comparison of the Strouhal evolution for a fixed blockage with previous experience [Grassi, 2002].
- Verification of the independence of Strouhal from Reynolds [Grassi, 2002].

Chapter 2

Experimental apparatus and set-up

In this chapter the laboratory equipment and the models used during the experimental activity are described as well as the different set-ups employed.

2.1 Wind tunnel

The different experiments are carried out in one of the wind tunnels available in Politecnico di Milano. In particular, the one used is the Sergio de Ponte wind tunnel. Some images of this tunnel are presented in the Figure 2.1.

(a) Wind tunnel entrance

(b) Test chamber of the wind tunnel

Figure 2.1: Sergio de Ponte wind tunnel

The Segio de Ponte tunnel is a closed return wind tunnel with a test section of 1000 mm $\times$ 1500 mm and a turbulence level of 0.01%.

The maximum wind speed is 55 m/s with a total power of 100 kW. This apparatus has 6 fans disposed in 2 columns of 3 fans. Furthermore, the plant has a centrifugal fan that blows air inside the tunnel in the inner part of the first corner after the test section. In this way the absolute pressure in the test section is controlled, in order to keep close to zero the pressure difference between inside and outside the test section. Several advantages come up from this null pressure difference:

- the load on the walls of the test section is reduced, which is particularly important since one of the walls is made up of crystal.
- the air flow through holes, openings and gaps on the walls is reduced. These vents are usually used for model supports, cables, etc., however the air flow which can go though them may interfere with measurements and disturb data obtained.

2.2 Models

Two different pairs of plates are used in the experiments, in order to produce different blockage ratios. As it can be observed in Figure 2.2b, the cross section of both plates is trapezoidal and, in this manner, the corners formed are sharp, which reduces the aerodynamic effects of the thickness of the plates.

The larger plate has a length of 1000 mm (equal to the length of the test section) with a chord of 140 mm and a thickness of 7 mm (see Figure 2.4a). On the other hand, smaller model has a length of 1000 mm with a chord of 70 mm and a thickness of 3.5 mm (see Figure 2.4b), thus the blockage ratio is half the one for the larger plate. In Figure 2.2a is visible that both models have the same length.

Unlike the experimental work performed by [Grassi, 2002], where the plates are crafted from an aluminum and titanium sandwich, for this work both plate models are made up of steel. Thus a high bending stiffness is achieved, which is of particular importance as during the experiments is vital to avoid vibrations. In fact, the natural frequency of the plate has been checked, by using an accelerometer, to be far from *vortex shedding* frequency in order not to interfere with the measurement of the last one.

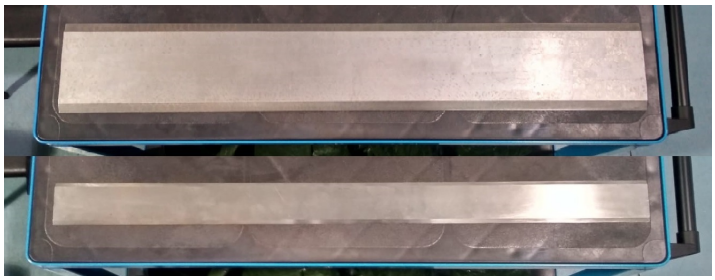

(a) The two different plate models: 140 mm chord (above) and 70 mm chord (below)

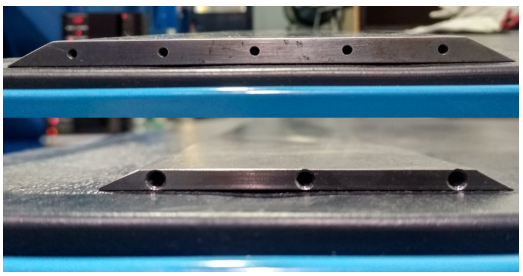

(b) Sections of larger plate (above) and smaller plate (below)

Figure 2.2: Comparison between the diffeerent plates used in laboratory

2.3 Measurement apparatus

For the purpose of measuring the velocity at the back of the downstream cylinder a hot wire anemometer (HWA) is used (see Figure 2.3a). In particular, the anemometer used is the *AA.LAB SYSTEMS LTD mod. AN-1003 CTA* (constant temperature) with internal signal conditioner, that is, filter and amplifier. The probe utilized for the anemometer is a *Dantec 55P11* general purpose straight single wire probe. All the measurements are taken with a overheat ratio [1] equal to 0.8.

For the placement of the anemometer a hollow carbon fiber tube is used as a support. This tube is connected to the roof of the test chamber by means of a rail (see Figure 2.3b), allowing the movement of the anemometer when the rear cylinder is displaced.

(a) Hot Wire Anemometer

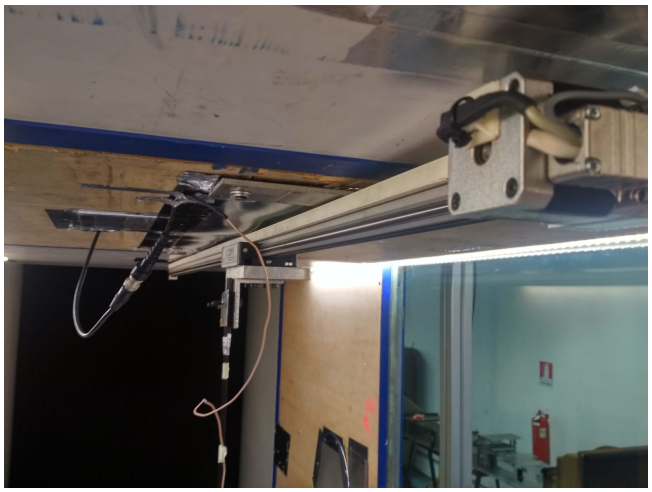

(b) Rail for the displacement of the HWA

Figure 2.3: Set-up of the probe system for experimental activity

[1] the overheat ratio is defined as the ratio between the electrical resistance of the wire at a ambient temperature and the resistance at operative conditions

For the signal acquisition process several devices of automated test equipment are used. The output analog signal from the anemometer, already amplified and filtered, goes into the *National Instruments NI 6284* placed in the data acquisition system *National Instruments NI PXI 1050*. The *NI 6284* is a 18 bit, 500 kS/s data acquisition device for voltage signals with an A/D converter. The already digitalized signal travels in the PXI bus and afterwards is transferred by means of an optical fiber to a PCI board (*NI PCI-8335 MXI-3*) in the computer.

Both the start of the acquisition process and a rough approach of the *vortex shedding* frequency are performed by means of *LabVIEW (Laboratory Virtual Instrument Engineering Workbench)*, a platform and development environment aimed at the design of systems.

2.4 Experimental set-up

In the Figure 2.4 the two different set-ups used in the experimental activity are depicted. The most important difference between them is the chord of the plates. As aforementioned, this difference allows to work with two different blockage ratios. For the measurement with single plate the anemometer is placed in the same position than for the rear plate in the corresponding set-up.

For the development of the experiments the upstream plate is fixed at the same position while the downstream one is displaced along the test chamber. Both plates are screwed to thin rectangular steel rods at their sides, minimizing in this way the flow disturbances and easing the displacement of the rear plate.

The displacement is carried out by means of the screwing of the plate supports to thick steel strips with holes along them located at the sidewalls of the test chamber (see Figure 2.5).

Considering the fixed plate position as origin of the horizontal distance, along the first 280 mm of the strips the holes are spaced by 7 mm. On the other hand, for the rest of the strips the holes are spaced by 35 mm.

For the plates of $c = 140$ mm the length of the test chamber allows to reach until a distance equal 6 c, whereas in the case of the small plates the maximum distance available for measurements is equal to 12 c.

The main goal of the measurements is to obtain the *vortex shedding* frequency, thus the signal acquired by the anemometer is analyzed by means of the application of the Fast Fourier Transform (FFT). This frequency analysis tool is introduced in the next chapter.

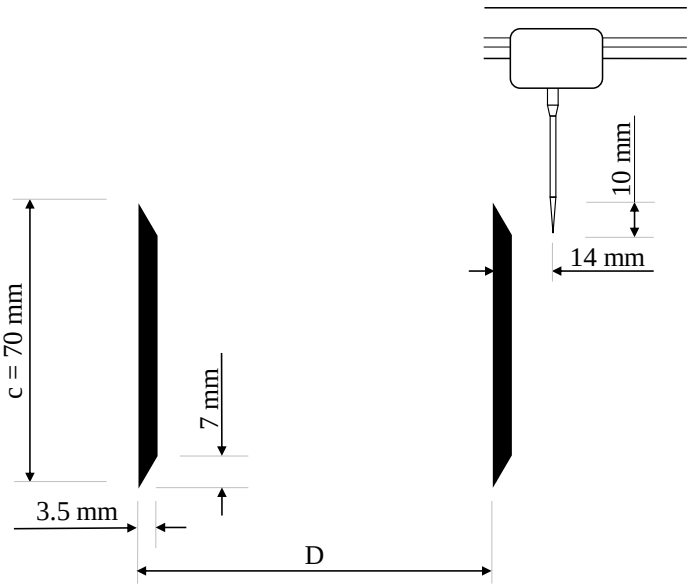

(a) Experiment set-up for 7 cm-chord plates in tandem

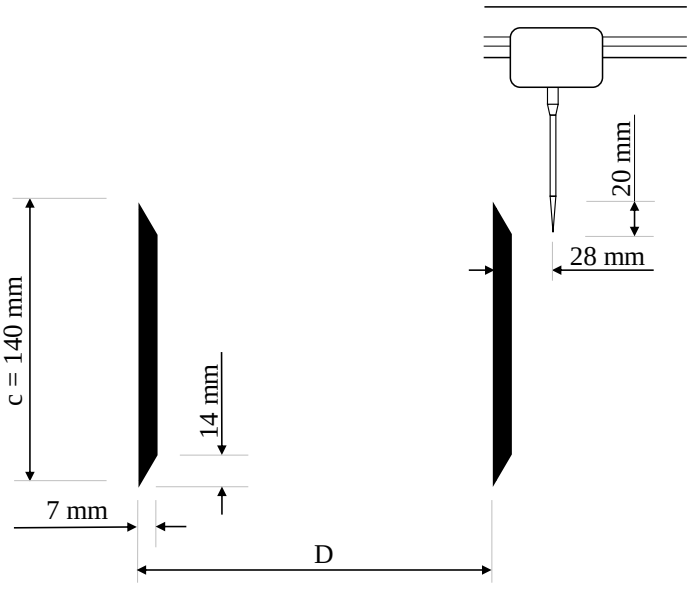

(b) Experiment set-up for 14 cm-chord plates in tandem

Figure 2.4: Set-ups for the two different tandem experiments

Figure 2.5: Metal strips at the sidewalls of test chamber and steel rod supports mounted for small plate measurements

Chapter 3

Analysis of signals

In order to accomplish a correct study of the measurements taken by the anemometer during the experimental stage is important to have a clear understanding of the type signal analysis utilized in this work.

The aim of taking measurements is to analyze them in order to obtain the main frequency of the velocity signal measured. The main frequency in this case corresponds to the frequency of vortex detachment. It is possible to get this frequency by means of the *Fourier analysis*.

A brief introduction to this kind of analysis is made in the following sections.

The Fourier series is a mathematical tool of Fourier analysis which allows to represent a continuous function $f(t)$ as a summation of sinusoids with different amplitudes and frequencies. Theses series are defined as follows:

$$f(t) = \frac{a_0}{2} + \sum_{n=1}^{\infty} \left[a_n \cos \frac{2n\pi}{T} t + b_n \sin \frac{2n\pi}{T} t \right] \tag{3.1}$$

Where a_0, a_n and b_n are the Fourier coefficients and have the following expressions:

$$a_0 = \frac{2}{T} \int_{-T/2}^{T/2} f(t)dt, \qquad a_n = \frac{2}{T} \int_{-T/2}^{T/2} f(t) \cos\left(\frac{2n\pi}{T} t\right) dt, \qquad b_n = \frac{2}{T} \int_{-T/2}^{T/2} f(t) \sin\left(\frac{2n\pi}{T} t\right) dt$$

This makes possible the analysis of the different frequencies of the function of study $f(t)$ and their weights in the aforementioned function. Nevertheless, this conversion to Fourier series is only possible if the function $f(t)$ is periodic. Otherwise, it is needed to go to the Fourier Transform.

The Fourier Transform (FT) allows to transform a continuous function $f(t)$ between the frequency domain and time domain. It is defined as follows:

$$\mathcal{F}[f(t)] = F(\omega) = \int_{-\infty}^{+\infty} f(t)e^{-2\pi ix\omega}dx \tag{3.2}$$

And the Inverse Fourier Transform (IFT) is:

$$\mathcal{F}^{-1}[F(\omega)] = f(t) = \int_{-\infty}^{+\infty} F(\omega)e^{2\pi ix\omega}d\omega \tag{3.3}$$

Through the use of this transform is possible to obtain the frequency spectrum of the function $f(t)$ and reconstruct the function from its spectrum by means the IFT. However, as mentioned before, this is only possible if the function is continuous. In the case of having discrete values of the function, which happens when measurements are taken in the laboratory, it inevitable to move to the Discrete Fourier Transform.

The Discrete Fourier Transform (DFT), likewise the previous mathematical tools, transforms signals between the frequency domain and time domain. Nevertheless, the signal of study has to be discrete and with finite length N_d. It is defined as:

$$X_k = \sum_{n=0}^{N_d-1} x_n e^{-\frac{2\pi i}{N_d}kn} \qquad k = 0, \ldots, N_d - 1 \tag{3.4}$$

And the Inverse Discrete Fourier Transform (IDFT) is:

$$x_n = \frac{1}{N_d}\sum_{k=0}^{N_d-1} X_k e^{\frac{2\pi i}{N_d}kn} \qquad n = 0, \ldots, N_d - 1 \tag{3.5}$$

Using this transform is possible to obtain the frequency spectrum of a discrete and finite-length signal, which is suitable for this work as the acquisition of signal provides discrete points of the signal.

The Fast Fourier Transform is simply the algorithm implemented to compute the DFT in a fast and efficient manner. Usually the term FFT is also use to denote the DFT, although they are different concepts. Hereinafter the term FFT is also taken to refer to the DFT.

3.1 Averaging multiple FFTs

During the calculation of the frequency spectra of the different signals acquired it is observed a significant level of noise and, thus, the location of the peak of frequency sought can be hindered. As a result, the averaging of multiple FFTs turns up.

This averaging method allows to mitigate the dificulties caused by the noise by reducing the noise variance of the DFT. Exist two types of averaging: *coherent avergaing* and *incoherent averaging* [Lyons, 2010]. The first type requires the collection of a set of signal samples with the same time phase at the beginning. On the other hand, the second one does not use sample timing constraints, that is, the different signal measurement intervals are not synchronized and, hence, the signal segments can be taken from one single signal measurement. Due to the excessive load of work that the first type would imply, the *incoherent averaging* is selected for the present work.

This FFTs averaging is usually combined with the use of overlapped consecutive segments. Thus, the procedure of the method can be described as follows:

1. The entire set of signal data is split into N segments and with M points overlapped between consecutive segments.

2. The FFT of each segment is computed.

3. The resulting FFTs points are added and the result is divided by the number of segments N, that is to say, the different FFTs obtained are averaged.

It is important to clarify that what is reduced is the variance of the noise and not the noise itself. The reduction of noise variance respect to the noise variance of the single FFT can be expressed with the following ratio [Welch, 1967]:

$$\frac{\sigma^2_{\text{N FFTs}}}{\sigma^2_{\text{single FFT}}} = \frac{1}{N} \tag{3.6}$$

It is observable in Equation 3.6 and Figure 3.1 that the larger the number of segments, the lower the noise variance is. In theory, the increase of numbers of segment would improve the obtaining of the frequency peak, however, if the number segments is increased the number of data points decreases and, as it can be observed in Equation 3.7, the frequency resolution is worsened.

$$\Delta f = \frac{f_s}{N_s} = \frac{1}{T} \tag{3.7}$$

where Δf is the frequency resolution, f_s the sampling frequency, N_s the number of data points of a signal segment and T the sampling time.

To avoid this loss in resolution the f_s may be increased, nevertheless, it entails taking new measurements which is not convenient if the number of measurements is large. Therefore, during the analysis of the signal utmost care must be paid to the number of segments the signal is divided in, seeking the best trade-off between frequency resolution and noise variance reduction.

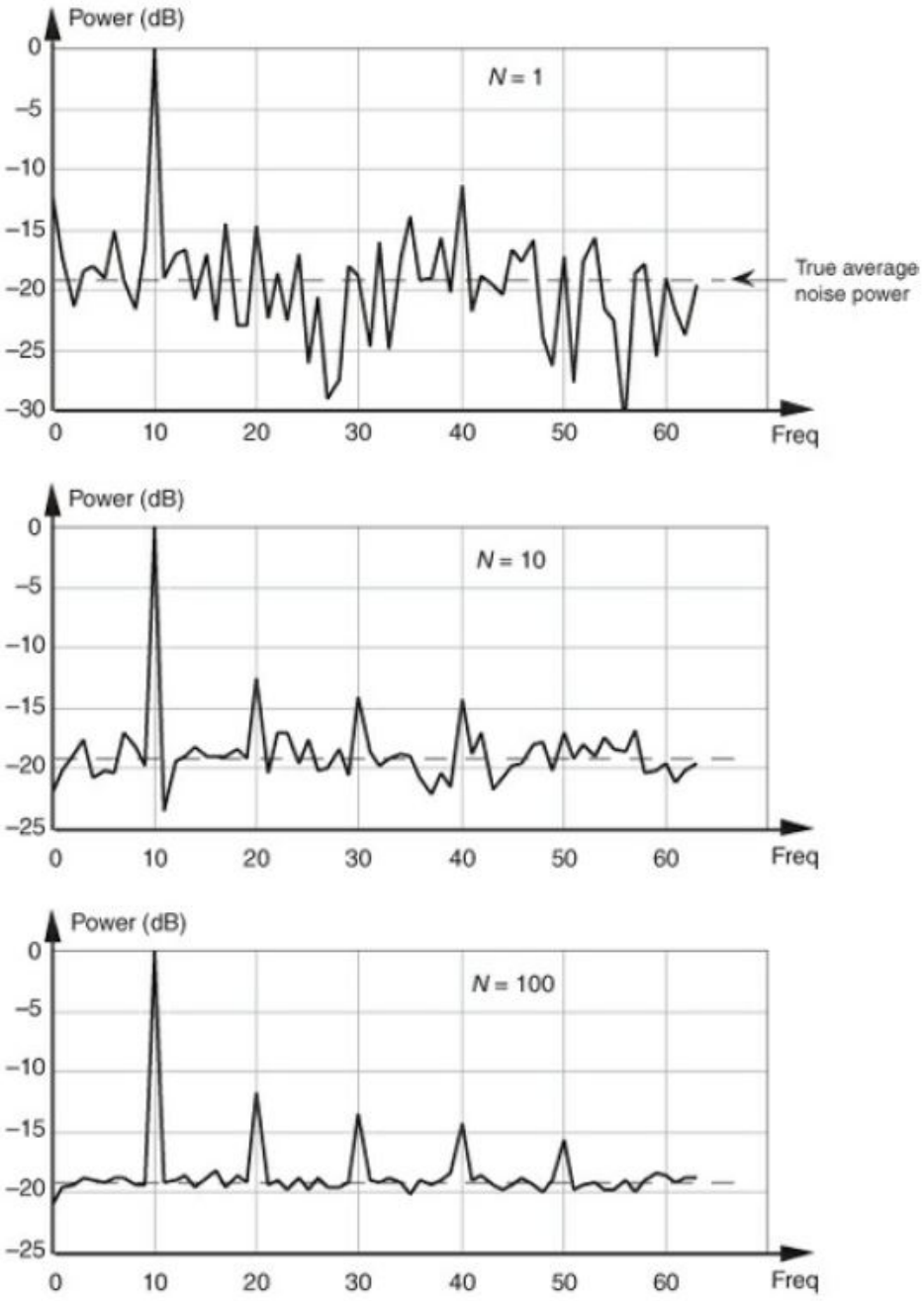

Figure 3.1: Averaging of a FFT with increasing number of segments N [Lyons, 2010]

3.2 Power Spectral Density

Another interesting diagram that can be useful in the signal analysis is the Power Spectra Density (PSD) representation. The power spectrum of a signal represents the power distribution among the different frequencies of the given signal. The PSD of a function $f(t)$ is defined as:

$$S_{xx} = |\mathcal{F}[f(t)]|^2 \tag{3.8}$$

In fact, this is the definition of a periodogram. Similarly to what seen in the previous section, the acquired signal can be split in several segments and then the different periodograms are averaged in order to diminish the error the noise may induce. One of the most famous methods for computing the PSD is the *Welch's method*. Its procedure is the following:

1. The entire set of signal data is split into N segments and with M points overlapped between consecutive segments.

2. Each signal segment is windowed and their PSDs are computed.

3. The resulting PSD points are added and divided by the number of segments N, in other words, the different PSDs are averaged.

The windowing of the data segments makes the *Welch's method* a *modified periodogram* method.

MATLAB has a function called `pwelch` which allows to compute the PSD by means of the *Welch's method* varying the segments length and the overlapping as desired. Hence, this computational tool is exploited in the present work for the analysis of the acquired signal.

Chapter 4

Results

In this chapter it is carried out the processing of the signals acquired during the laboratory activity as well as the comparison between results obtained for the different cases tested, focusing in the effect the blockage has on Strouhal and difference with previous experience.

In literature it has been shown that the blockage ratio considerably affects the aerodynamics forces and *vortex shedding* behavior [West and Apelt, 1982]. The blockage ratio is defined as follows:

$$k = \frac{\text{Frontal area of Model}}{\text{Cross-section area of test section}} \cdot 100\% \tag{4.1}$$

For the cases of study, since the plate length and test chamber width are equal, this ratio is reduced to the ratio between the chord of the plate and the height of the test section.

The main goal of the work is the evaluation of the Strouhal behavior varying the distance between plates. The Strouhal number is defined as:

$$St = \frac{fL}{U} \tag{4.2}$$

where f is the *vortex shedding* frequency, L is the characteristic length and U is the free-stream velocity.

In order to have a robust reference for Strouhal number, in literature is available the correction formula introduced by [Ota et al., 1994]:

$$St_{cor} = \frac{0.136}{1 - 1.21k} \tag{4.3}$$

where St_{cor} is the literature Strouhal and k the blockage ratio of the experiment case.

Since this correction formula is based in flow around one single body, these corrected Strouhal numbers are used as a reference for only the Strouhal obtained for single plate cases.

For the computation of the Strouhal for a given case, the velocity measurements taken for that particular case are used. From the analysis of the content in frequency of this data it can be obtained the main frequency f, which corresponds to the frequency with largest peak in the FFT. For its part, the velocity U is calculated as the mean of the different velocities values measured for the specific case. Once these variables are computed and knowing that the characteristic length of a plate is its chord, the Strouhal is readily determined.

4.1 Measurements with 9.33% blockage ratio

In this section it is described the processing of the measurement data obtained for the plates of chord $c = 140$ mm. With this chord of plate it is achieved a blockage $k = 9.33\%$, which is fiarly close to the one in literature experience $k = 10\%$[Grassi, 2002]. Thus, the results here obtained, apart from contrasting them to the ones of lower blockage, can be also compared to this previous work and verify if there are discrepancies between them.

For the experiment it is used a sampling frequency f_s of 1000 Hz and a sampling time T of 100 s. Thus, the frequency resolution Δf has a value of 0.01 Hz (Equation 3.7).

The Reynolds number used during this experiment is selected so it can be compared to previous experience. In this case it is selected $Re = 22400$ and, hence, the velocity induced by wind tunnel is 2.3 m/s.

The first step in the measurement activity is to measure the Strouhal of the isolated plate, in order to have a reference value and normalize the values obtained with the tandem arrangement. Since the St for single plate is also affected by the blockage, a normalization with respect to this Strouhal is done in order to isolate the effect of the blockage within the tandem results.

The measurements for the tandem set-up are carried out by displacing the downstream plate respect to the fore plate and measuring the velocity at the back of the rear body.

The initial position is 0.5 D/c, where D is the spacing between plates. From this origin the distance is increased by 0.1 D/c each time until it is reached 1.4 D/c. From this point until 2.0 D/c the distance is incremented by 0.05 D/c. These small distance steps are selected as it is predicted the presence of marked variation of the Strouhal within this region. From 2.0 D/c to 6.0 D/c the distance step is 0.5 D/c, since the expected Strouhal variation is smoother than in the previous zone.

For the zone with abrupt evolution of Strouhal several measurements are taken, whereas for larger distances generally is taken one measurement per position.

Nevertheless, before representing the results it is necessary to process the measurement data. When computing the FFTs of the measurement data some noise is found and this can lead to misleading results for f. Therefore, it is convenient to average the FFT, reducing the noise variance, and, simultaneously, keep a suitable Δf in order to acquire a frequency f as close as possible to a reference value.

The averaging FFT process depends, as seen in Section 3.1, on two parameters: the size of signal segments N and the number of overlapped points M. Therefore, a parametric study is performed in order to find those parameter values which allow to get the most correct Strouhal with high accuracy and cleanness of the frequency spectra.

This above-mentioned study is performed with the function `pwelch`, provided by MATLAB, and the developed function `fftavg` (Figure 4.1), selecting the one which shows the most adequate results.

In Figure 4.1 it can be found the `fftavg` function code developed in MATLAB environment to compute the average of multiple FFTs. This code has been elaborated according to the steps described in Section 3.1.

```
function [XT,f]=fftavg(x,bindim,nshft,fs)
%=========================================================================
% Function to compute the averaged Fast Fourier Transform of the vector x
% (sampled at 'fs' Hz) using segments of size 'bindim' and shift of 'nshft'
% points between segments
%=========================================================================

L=length(x);
X=1/bindim*(abs(fft(x(1:bindim))));
X(2:end-1)= 2*X(2:end-1);
XT=X;
i=nshft+1;
while 1
    next=1/bindim*abs(fft(x(i:i+bindim-1)));
    next(2:end-1)= 2*next(2:end-1);
    XT=[XT; next];
    i=i+nshft;
    if i>L-bindim+1
        break
    end
end
s=size(XT);
XT=sum(XT)/s(1);
f= fs/bindim*(0:bindim-1);

end
```

Figure 4.1: Function developed in MATLAB for averaging multiple FFTs

For this function `fftavg` the overlapped data points M is not a input, but the shift of points is. From the relation shown in Equation 4.4 it is observable that the number of overlapped points is readily retrieved.

$$M = N_s - \delta \tag{4.4}$$

where δ is the shift of points between two consecutive signal segments.

Furthermore, the width w of the signal segments is the other input for `fftavg`, instead of the number of signal segments N.

However, unlike `fftavg`, `pwelch` computes the Power Spectral Density of the data acquired. Despite this difference, both are tools that allow to obtain the main frequency of the signal measured and, consequently, their outputs can be compared. `pwelch` also has as input the width w of the segments, though its other input is the number of overlapped points M.

As the single plate Strouhal is the used to normalize the tandem Strouhal, this first number is the most significant value and, therefore, the most suitable for the averaging FFT parameter study. Once calculated these parameters, they are also used for the tandem cases.

4.1.1 Measurements of single plate

By using the correction formula for blockage (Equation 4.3), the literature Strouhal for the single plate is:

$$St_{cor} = 0.1533$$

For this study several values of w with 50% overlap are tested. As result, the values selected are $w = 50000$ and $\delta = 25000$ for the `pwelch` function. From Table 4.1 it is observed that with these values the frequency resolution is high (0.02 Hz) and the frequency spectrum is clearer than the one computed by means of `fftavg`.

	Frequency (Hz)	Strouhal number	Relative error (%)
Literarture reference	-	0.1533	0
`fftavg`	2.50	0.1480	3.4780
`pwelch`	2.58	0.1527	0.3892

Table 4.1: Comparison of St and relative error obtained with $w = 50000$ and $\delta = 25000$ using PSD and FFT diagrams for $k = 9.33\%$

In addition, the relative error shown by the selected parameters and function in Table 4.1 is low, confirming the correctness of the choice made.

Once selected parameters and function for the computation of Strouhal, the shift is decreased to analyze the reduction of error it can provide. Nevertheless, it is noticed that the noise variance is not reduced largely and the δ remains as the half of the segment. In this way the computation time is not increased and at the same time the accuracy is kept unchanged.

Therefore, the St for the single plate is:

$$St_{ref} = 0.1527$$

4.1.2 Measurements of plates in tandem

As mentioned before, the Strouhal computation for tandem cases is carried out with the same parameters than in isolated plate.

Some PSD diagrams corresponding to tandem cases can be found in Figure 4.2.

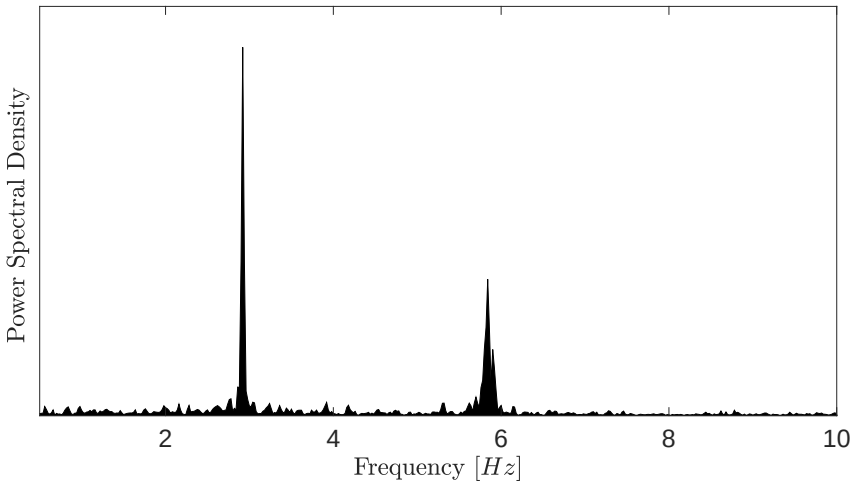

(a) PSD for separation distance 1.55 D/c

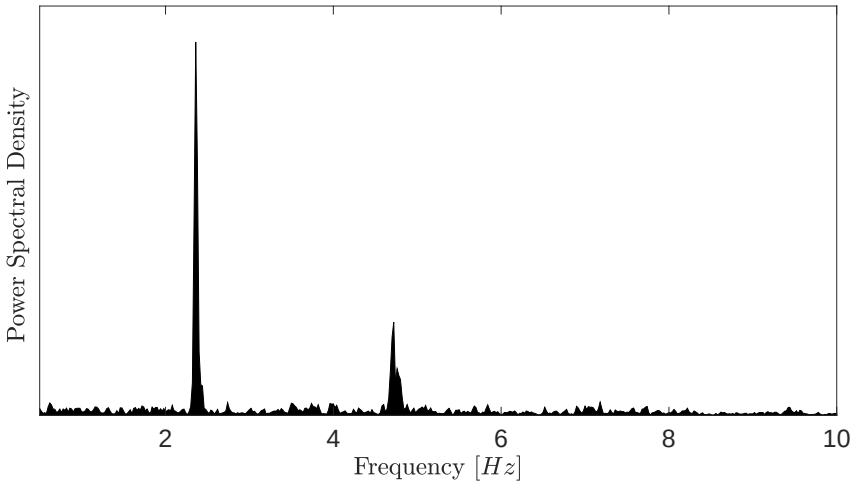

(b) PSD for separation distance 3.0 D/c

Figure 4.2: PSD diagrams for different distances in tandem arrangement and $k = 9.33\%$

It is observed that apart from the main frequency peak found in the PSD diagrams there is a second peak at a high frequency with lower amplitude. This secondary peak is just the multiple of a main frequency and not the frequency of another flow mode which would indicate the existence of bistability.

Finally, the normalized Strouhal evolution obtained for this blockage ratio is shown in Figure 4.3.

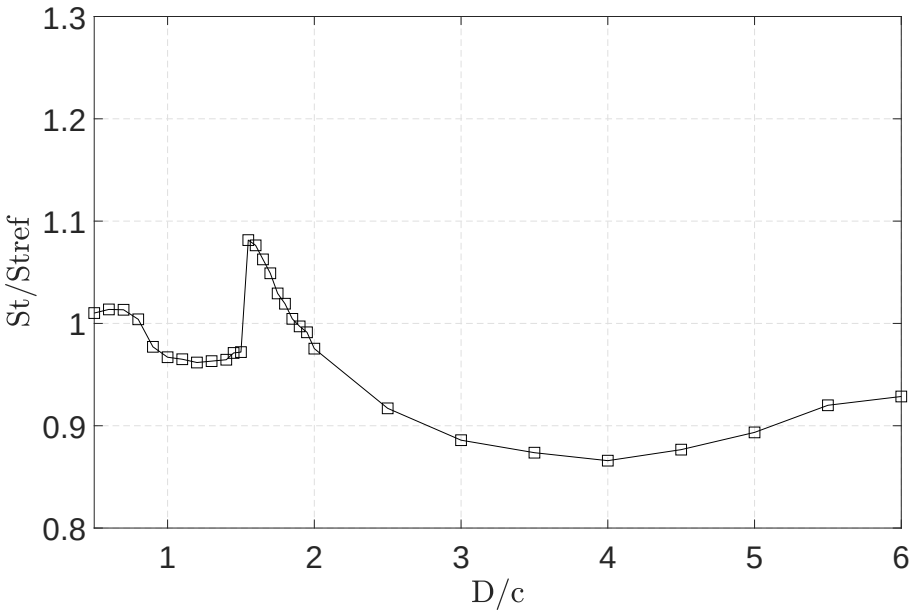

Figure 4.3: Normalized Strouhal evolution with respect to separation distance for $k = 9.33\%$

4.2 Measurements with 4.66% blockage ratio

Within this section the processing of the data acquired for the plates of $c = 70$ mm is carried out. By using a plate with half the chord of the previous section plate the blockage ratio obtained is, indeed, also the half of the first experiment blockage, that is, $k = 4.66\%$. From comparing the evolution of Strouhal for both blockage ratios, it can be made an estimation of the effect of this ratio on the wake behavior.

The sampling settings for this set of experiments remains the same: sampling at $f_s = 1000$ Hz and during a time $T = 100$ s, achieving a frequency resolution Δf of 0.01 Hz.

The Reynolds number is kept the same than in larger k case. However, as the chord of the plate has changed, the velocity set in the wind tunnel must be also varied. Therefore, it follows that the velocity induced by the wind tunnel has to be 4.6 m/s.

Similarly to larger plates, the separation jumps between measurements is small around the zone with expected rough changes of Strouhal and large in the region furthest from the fixed plate. Thus, the measurements start with spacing equal to 0.5 D/c until reaching 2.0 D/c with a increment of 0.1 D/c. Once finished this first region, the spacing increase is changed to 0.5 D/c. With this new increment the downstream plate is displaced up to 12 D/c.

The measurements within the most sensitive zones are repeated at least once in order to minimize the probabilities of working with inaccurate measurements.

Before representing Strouhal evolution, is necessary again to perform a parametric study in order to find the most appropriate parameters w and δ and function for Strouhal computation with this new blockage.

4.2.1 Measurements of single plate

With the blockage ratio of this plate, the literature Strouhal is:

$$St_{cor} = 0.1441$$

As done before, the study of parameters is carried out with several pairs of values w and δ, always keeping an overlap of 50%. However, during this analysis it is observed that increasing w from a segment width of 10000, thereby increasing also Δf, leads for both FFT and PSD diagrams to the same frequency peak and, hence, the same Strouhal (see Table 4.2). In order to select the most suitable parameter it is preferred to have a high resolution and obtain a Strouhal number close to the Strouhal of literature. Nevertheless, as it can be noticed that for both studied functions the frequency spectrum is noisier with $w = 50000$ than for $w = 40000$. Therefore, the parameters selected are $w = 40000$ and $\delta = 20000$.

As `fftavg` and `pwelch` show the same performance for these chosen parameters, it is necessary to analyze them to discard one. In this case it is noted that the PSD diagram shows lower noise.

	Frequency (Hz)	Strouhal number	Relative error (%)
Literarture reference	-	0.1441	0
w=40000, δ=20000			
`fftavg`	9.5	0.1378	4.4006
`pwelch`	9.5	0.1378	4.4006
w=50000, δ=25000			
`fftavg`	9.5	0.1378	4.4006
`pwelch`	9.5	0.1378	4.4006

Table 4.2: Comparison of St and relative error obtained with $w = 40000$, $\delta = 20000$ and $w = 50000$, $\delta = 25000$ using PSD and FFT diagrams for $k = 4.66\%$

Besides, in Table 4.2 it is noticed the low relative error achieved with the selected parameters and function, confirming the wise choice of parameters.

Once PSD calculation is selected for the computation of Strouhal reference, the shift is decreased in order to reduce the noise of the PSD diagram. However, the noise is not reduced at a high level so the shift remains the half of the length of the segment, that is, 50% overlap, to reach an adequate trade-off between computation time and reduction level of noise variance.

Hence, the Strouhal for single plate is:

$$St_{ref} = 0.1378$$

4.2.2 Measurements of plates in tandem

In Figure 4.4 some diagrams of Power Spectral Density calculated for different separations are shown.

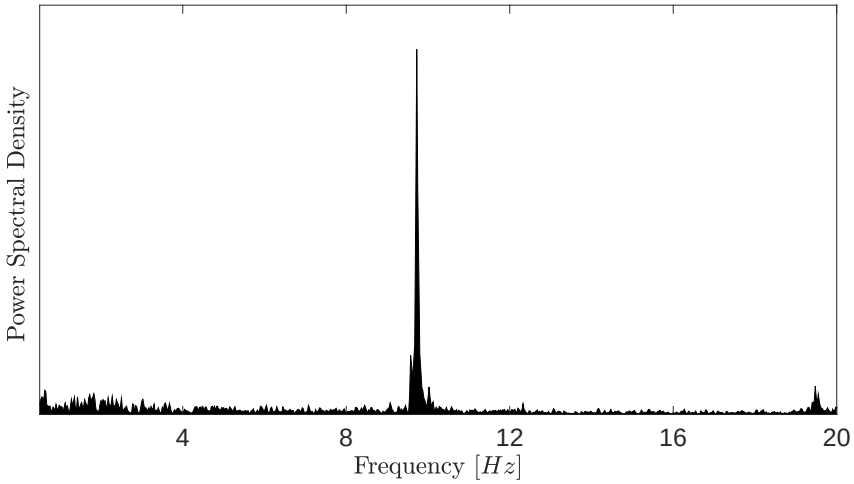

(a) PSD for separation distance 1.0 D/c

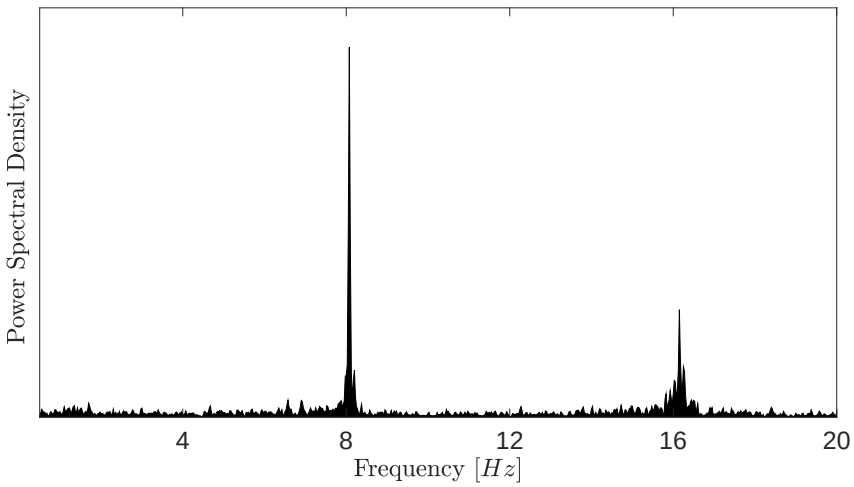

(b) PSD for separation distance 4.5 D/c

Figure 4.4: PSD diagrams for different distances in tandem arrangement and $k = 4.66\%$

Similarly to the case of larger plates, a secondary peak is observed in the PSD diagrams. However, these peaks are those corresponding to the multiples of the main frequencies and do not represent the frequency of another flow mode.

The Strouhal evolution properly calculated for this blockage is represented in Figure 4.5.

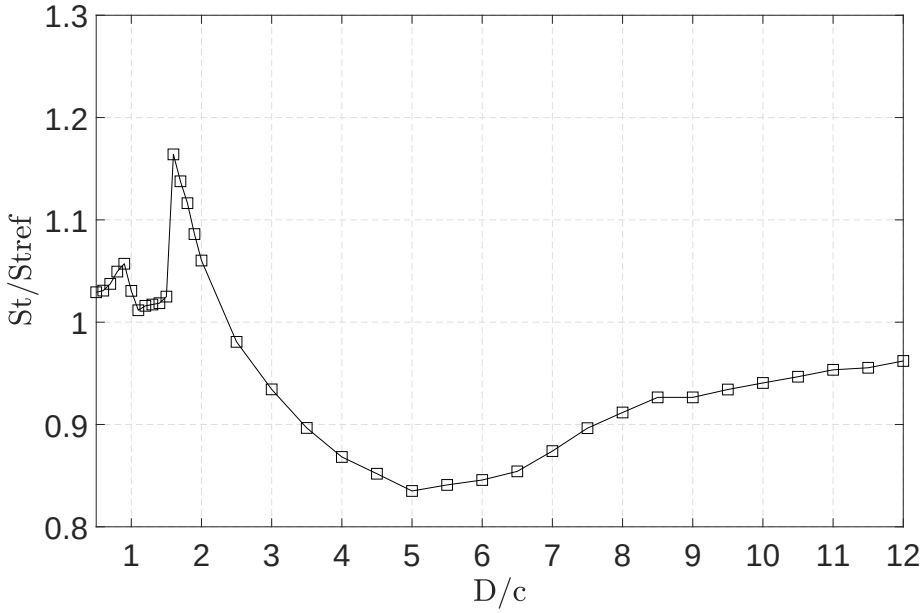

Figure 4.5: Normalized Strouhal evolution with respect to separation distance for $k = 4.66\%$

4.3 Comparison of results

In this section three different comparison are made. Firstly, the comparison between the Strouhal plots at different blockage ratios and then the comparison between the Strouhal trend here obtained and the one obtained by [Grassi, 2002], which are calculated at quite similar blockages. Finally, the Strouhal plot for the 9.33% blockage is compared with the results obtained for the same blockage but higher Reynolds.

In Figure 4.6 the blockage effect is clearly visible. In the first zone, from 0.5 D/c to 1.6 D/c, it is noticeable that, despite both curves show the same shape, the normalized Strouhal for lower blockage takes higher values. It is remarkable that the peak reached at 1.6 D/c by the lower blockage ratio is larger than the peak associated with higher blockage.

From this peak point until reaching the minimum Strouhal for 9.33% blockage, both curves show a decreasing behavior. The curve for higher blockage starts to increase its slope until it gets zero value at its minimum. However, the lower blockage curve shows only a slight increase of slope and continues decreasing until 5 D/c, showing lower minimum and a clear delay of Strouhal trend with respect to larger blockage case.

From their respective minimums, both Strouhal increase until approximating asymptotically to the value of S_{ref}, though the Strouhal for 4.66% blockage shows a smaller increasing rate.

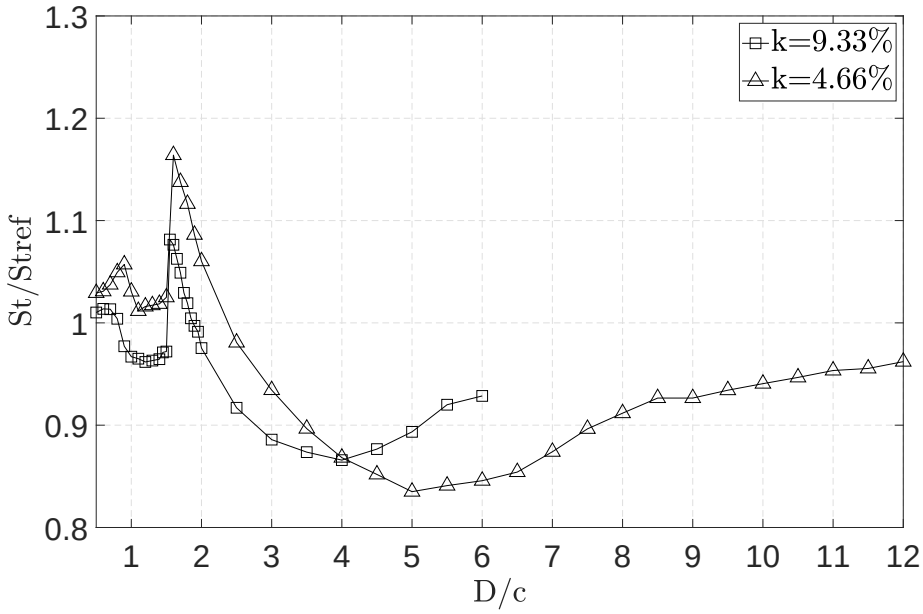

Figure 4.6: Comparison of Strouhal evolution between $k = 9.33\%$ and $k = 4.66\%$

Looking the comparison with previous work, the differences between trends in Figure 4.7 are also easily noticeable. In the first points the discrepancies are not very large, however it is observed that their respective peaks are reached at very different distances and have different values, being the peak for the present experience lower. The peak reached by the data of previous work is located at 1.0 D/c whereas the peak of the other curve is found at 1.55 D/c.

Apart from this difference, both Strouhal evolutions show the same behavior: they decrease until similar minimum at alike separation distance and then both increase and approximate asymptotically to their respective St_{ref} with comparable slope.

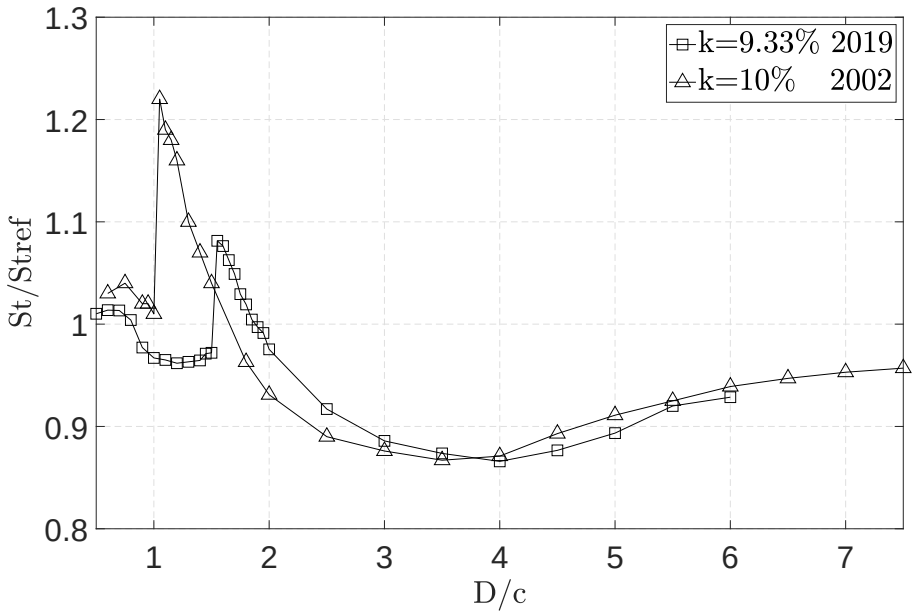

Figure 4.7: Comparison of Strouhal evolution between $k = 9.33\%$ (2019) and $k = 10\%$ (2002)

Finally, for the last comparison showed in Figure 4.8 the results for different Re are almost the same despite some small discrepancies at lower spacings. Therefore, the Reyndols independence for flat plates stated by [Grassi, 2002] is verified.

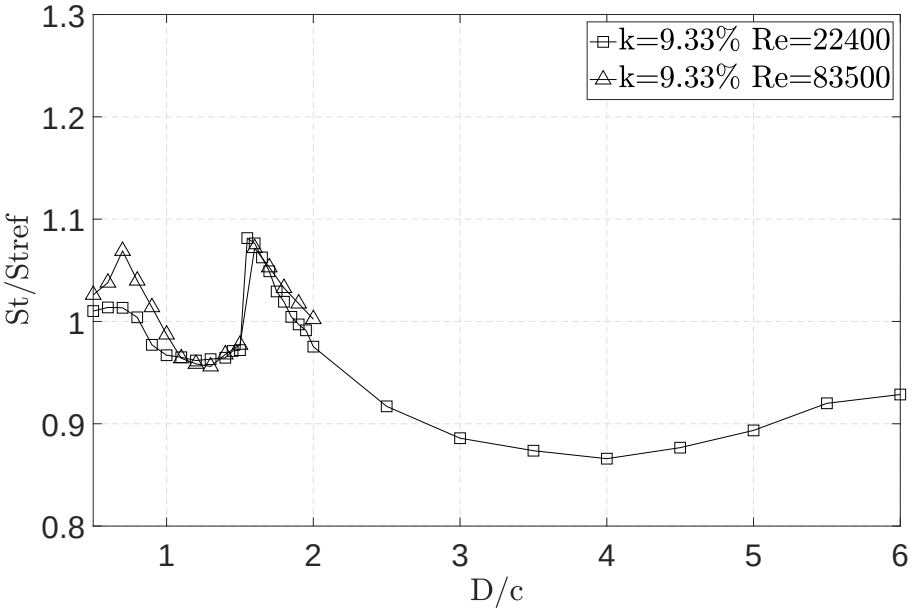

Figure 4.8: Comparison of Strouhal evolution between $Re = 22400$ and $Re = 83500$ for $k = 9.33\%$

Chapter 5

Conclusions

During the development of this work experimental activity has been carried out in a wind tunnel in order to obtain the Strouhal evolution with respect to separation distance of flow around normal flat plates in tandem configuration at different blockage ratios.

It is essential to completely understand the effect blockage has on the Strouhal evolution and in this way avoid the acceptation of misleading results. The blockage effect is important in wind tunnel experiments since the less negligible the blockage is, the further the aerodynamic behavior is from the free stream one.

In order to carry out the Strouhal study it must be obtained the most accurate *vortex shedding* frequency. For this purpose it is performed a post-processing during which the capabilities of the FFT and PSD functions are compared and a parametric study is conducted to obtain the most precise Strouhal evolution. The selected parameters minimize the noise and provide a clean frequency spectrum. Afterwards, it is confirmed the right choice by checking that the relative error with respect to literature Strouhal is low.

For the results showed for different blockage ratios, a clear difference is found between Strouhal trends. The Strouhal for the lower blockage shows larger values than the one of the other blockage at low separation distances and a higher peak. After the peak, the curve for the lower blockage shows a slower evolution than 9.33% blockage, reaching minimum value and approximating in a asymptotic way to the St_{ref} later.

Some noticeable discrepancies are found between the present work and data from past work of [Grassi, 2002] for the similar blockage but in different wind tunnel. The data of the previous experience present a peak larger and before the present Strouhal evolution. After their respective peaks both curves show the same behavior, as they go asymptotically in the same manner.

Furthermore, another important difference between these Strouhal evolutions is the non-existence of bistability phenomenon in the results obtained in this project.

Although the blockage ratio is kept approximately the same between both experiments, the results obtained show clear differences. The difference in k is so small that it could not represent the entire effect which produces the discrepancies. Therefore, it is hypothesized that the environment of the wind tunnel, such as the turbulence level and the three-dimensionality, should produce an important effect.

The turbulence level of the wind tunnel used during the work of [Grassi, 2002] is three times the one of the wind tunnel employed in the present experience. Hence, the level of turbulence could have effect in the aerodynamic features related to *vortex shedding* studied in this work.

Moreover, in the previous experience the aspect ratio AR is half of the present one due to the use of a different wind tunnel and, thus, the three-dimensionality of the flow could have an effect on the Strouhal behavior.

And finally, regarding the experiments carried out at larger Reynolds and blockage equal to 9.33% it is observable that the increase in Reynolds does not affect to the Strouhal evolution, verifying the independence on Reynolds indicated by [Grassi, 2002].

Chapter 6

Recommendations for further work

In this chapter some suggestions for future works related to the blockage effect on the Strouhal for flat plates in tandem are addressed.

As mentioned before, the turbulence level can be a factor of high influence on Strouhal. In order to study its effect, the blockage must be kept constant while the turbulence level is changed by using a different wind tunnel.

A parameter to have into account in order to better evaluate the three-dimensionality of the flow is the aspect ratio AR. Whereas the blockage is kept constant, the aspect ratio is varied and similar to what occurs with previous point, the study with AR as a parameter is cumbersome. In order to isolate blockage and aspect ratio it would be necessary to change the size of the wind tunnel section or to have a wind tunnel with variable test section dimension.

A fast way of carrying out these two different studies is by means of the CFD. The turbulence level can be changed much easier in the CFD environment than in real experiments. Regarding to the three-dimensionality study, it can be addressed by computing the 2D and 3D cases separately and then comparing the differences between them.

Bibliography

[Auteri et al., 2009] Auteri, F., Belan, M., Cassinelli, C., and Gibertini, G. (2009). Interacting Wakes of Two Normal Flat Plates: An investigation based on phase averaging of LDA signals. *Journal of Visualization*, 12:307–321.

[Auteri et al., 2008] Auteri, F., Belan, M., Gibertini, G., and Grassi, D. (2008). Normal flat plates in tandem: An experimental investigation. *Journal of Wind Engineering and Industrial Aerodynamics*, 96:872–879.

[Awbi, 1983] Awbi, H. B. (1983). Effect of blockage on the Strouhal number of 2D bluff bodies. *Journal of Wind Engineering and Industrial Aerodynamics*, 12:353–362.

[Chen and Fang, 1996] Chen, J. M. and Fang, Y.-C. (1996). Strouhal numbers of inclined flat plates. *Journal of Wind Engineering and Industrial Aerodynamics*, 61:99–112.

[Fage and Johansen, 1927] Fage, A. and Johansen, F. C. (1927). On the flow of air behinf an inclinde flat plate of infinite span. In *Reports and memoranda*, volume 1104.

[Grassi, 2002] Grassi, D. (2002). Corrente vorticosa prodotta da due lamine piane in tandem. Bachelor's degree Thesis.

[Havel et al., 2001] Havel, B., Hangan, H., and Martinuzzi, R. (2001). Buffeting for 2D and 3D sharp-edged bluff bodies. *Journal of Wind Engineering and Industrial Aerodynamics*, 89:1369–1381.

[Igarashi, 1981] Igarashi, T. (1981). Characteristics of the flow around two circular cylinders arranged in tandem (1st report). *JSME International Journal Series B*, 24:323–331.

[Igarashi, 1984] Igarashi, T. (1984). Characteristics of the flow around two circular cylinders arranged in tandem (2nd report). *JSME International Journal Series B*, 27:2380–2387.

[Liu and Chen, 2002] Liu, C.-H. and Chen, J. M. (2002). Observations of Hysteresis in flow around two square cylinders in a tandem arrangement. *Journal of Wind Engineering and Industrial Aerodynamics*, 90:1019–1050.

[Luo et al., 1999] Luo, S. C., Li, L. L., and Shah, D. A. (1999). Aerodynamic stability of the downstream of the two tandem square-section cylinders. *Journal of Wind Engineering and Industrial Aerodynamics*, 79:79–103.

[Lyons, 2010] Lyons, R. G. (2010). *Understanding Digital Signal Processing*. Pearson Education, third edition.

[Ota et al., 1994] Ota, T., Okamoto, Y., and Yoshikawa, H. (1994). A correction formula for wall effects on unsteady forces of two-dimensional bluff bodies. *Journal of Fluids Engineering*, 116.

[Sarpkaya, 1975] Sarpkaya, T. (1975). An inviscid model of two-dimensional vortex shedding for transient and asymptotically steady separated flow over an inclined plate. *Journal of Fluid Mechanics*, 68:109–128.

[Takeuchi, 1990] Takeuchi, T. (1990). Effects of geometrical shape on vortex-induced oscillations of bridge tower. *Journal of Wind Engineering and Industrial Aerodynamics*, 33:359–368.

[Welch, 1967] Welch, P. D. (1967). The Use of Fast Fourier Transform for the Estimation of Power Spectra: A Method Based on Time Averaging Over Short, Modified Periodograms. *IEEE Transactions on Audio and Electroacoustics*, 15:70–73.

[West and Apelt, 1982] West, G. S. and Apelt, C. (1982). The effects of tunnel blockage and aspect ratio on the mean flow past a circular cylinder with Reynolds numbers between 104 and 105. *Journal of Fluid Mechanics*, 114:361–377.

[Xu and Zhou, 2004] Xu, G. G. and Zhou, Y. (2004). Strouhal numbers in the wake of the inline cylinders. *Experiments in Fluids*, 37:248–256.

[Zdravkovich, 1977] Zdravkovich, M. M. (1977). Review of flow interference between two circular cylinders in various arrangements. *Journal of Fluids Engineering*, 99:618–633.